Journal of Materials Chemistry C

Accepted Manuscript

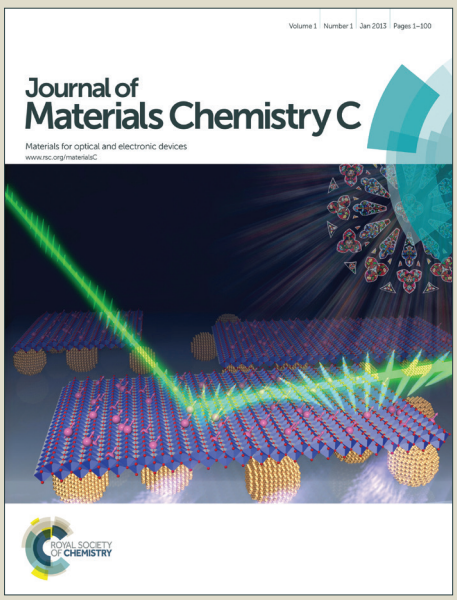

ROYAL SOCIETY OF CHEMISTRY

www.rsc.org/materialsC

Study on molecular distribution of organic composite films by combining photoemission spectroscopy with argon gas cluster ion beam sputtering

Dong-Jin Yun, JaeGwan Chung, Seong Heon Kim, Yongsu Kim, Minsu Seol, Jongwon Chung*, Sung-Hoon Park*

Analytical Science Laboratory of Samsung Advanced Institute of Technology

Maetan 3-dong, Yeongtong-gu, Suwon-si, Gyeonggi-do 443-803, Republic of Korea

* Corresponding author

Tel.: 82 31280 8436; E-mail: leo.park@samsung.com & jw0903.chung@samsung.com

2nd revision Submitted to Journal of Materials Chemistry C

Sep. 22, 2014

Abstract

X-ray/ultraviolet photoelectron spectroscopy (XPS/UPS) and argon gas cluster ion beam (GCIB) sputtering were combined to directly study the molecular configurations of organic composite films consisting of more than two different materials. In contrast to Ar ion sputtering, Ar GCIB sputtering does not critically distort the chemical states and atomic compositions of organic materials; therefore, this promising method enables the chemical structures of uncontaminated bulk regions and air-exposed surface regions of organic materials to be precisely examined. Hence, the molecular configurations of single-wall and multiwall carbon nanotube (SWNT and MWCNT) films, composed of corresponding CNTs and surfactants, could be specifically characterized based on the chemical state transitions in the C 1*s* core level depth profiles. Further, the XPS/UPS spectra showed variations in the chemical states with increasing sputtering time, which were fully consistent with the surface morphologies observed in the high-resolution atomic force microscopy and high-resolution secondary electron microscopy images. Hence, we believe that combining XPS/UPS with Ar GCIB sputtering can be an excellent method of investigating the molecular distributions of organic composite films.

1. Introduction

For decades, many research groups from a wide range of fields have studied organic electronics as a substitute for conventional silicon-based ones because of their material and process cost advantages. More and more organic electronic devices including organic thin-film transistors (OTFTs), organic photovoltaics (OPVs), dye-sensitized solar cells (DSSCs), and organic light-emitting diodes (OLEDs) increasingly require highly functionalized organic materials to replace the inorganic or metal component because of low cost and simple processing[1-4] However, unlike the film properties of inorganic materials, those of organic

ones are easily damaged by ion, plasma, or heat treatment; therefore, numerous difficulties are encountered using conventional processes to characterize the physical/chemical composition and other properties of organic-based materials,[5,6] and argon-ion-sputtering-induced damage to the chemical/electrical states of organic materials is a typical example.[5-7] Until now, ultraviolet photoemission spectroscopy (UPS) and X-ray photoemission spectroscopy (XPS) have been most commonly used to characterize the chemical bonding states, orientations, and compositions of the surface regions of organic/inorganic materials.[7-9] The properties of the surface region of most materials are different from those of the bulk because of contamination, chemical reactions, dangling bonds, and exposure to the environment or air.[8,9] Therefore, most photoemission spectroscopy (PES) equipment uses argon (Ar) ion sputtering depth profiling to study the chemical state of the bulk region.[5,6] However, despite advantages such as high sputtering yield, low cost, and ease of control, Ar ion sputtering degrades or destroys the surface chemical bonding of some materials and can significantly skew the chemical state or the atomic composition of organic materials in particular. Hence, it has been almost impossible to use PES in order to accurately obtain chemical information about the bulk or interface regions.[5-7]

The degradation of organic materials has been significantly reduced with the recent introduction of the Ar gas cluster ion beam (Ar GCIB) sputtering system, thereby enabling PES to be used in order to study the bulk, interface, and surface properties of organic materials.[6,7,10,11] Especially, according to various research reports, the Ar CCIB sputtering system allows of drastically minimizing the degradation and changes on the chemical states of organic materials due to the low energy per Ar atom used in this process, which is 100–1000 times lower than that in the Ar ion sputtering process.[6,7,10,11] Our experimental design clearly determined whether combining PES with Ar GCIB sputtering critically damaged the electronic structure of organic materials.[6,7,11] The chemical states and energy-level alignments

of small organic molecules such as pentacene and phenyl-c71-butyric-acid-methyl ester were well preserved even after repeated Ar GCIB sputtering.[7,11] The chemical/electronic structures of various structures of organic small molecules have been actively studied and the little effects of Ar GCIB sputtering process on them were clearly verified. However, up to now, there is few in-depth studies of the solution based composite polymer or bulk hetero-structure using Ar GCIB sputtering process. Considering the reliable results obtained for the organic layered structures, we believe that PES combined with Ar GCIB sputtering enables the molecular distributions of organic heterojunction or composite films to be directly characterized owing to the synergy between PES depth resolution (< 10 nm) and nondestructive Ar GCIB sputtering.[6,7,11]

In this work, the molecular distributions of spin-coated carbon nanotube (CNT) composite films, consisting of a surfactant and CNT strands, were directly investigated by combining PES with Ar GCIB sputtering. In addition to the primary analysis results of the XPS/UPS depth profiles, the film morphologies corresponding to various Ar GCIB sputtering conditions were examined using high-resolution optical microscopy (HR-OM), high-resolution atomic force microscopy (HR-AFM), and high-resolution secondary electron microscopy (HR-SEM) to clearly determine whether this method accurately provided information about the molecular distributions of organic composite films.

2. Experimental

Commercial multiwall and single-wall carbon nanotube (MWCNT and SWNT) inks (~1 wt%), containing metallic CNTs and organic surfactants dispersed in aqueous solvents, were used to prepare MWCNT and SWNT films. The SiO_2 (300 nm)/N++Si substrate was cleaned using piranha solution, and CNT ink was spin-coated onto the substrate rotating at 1000 rpm. The coated substrate was then dried in a vacuum oven at 100°C for 1 h.

H_2SO_4-treated SWNT and poly(3,4-ethylenedioxythiophene):poly(styrenesulfonate) (PEDOT:PSS) films were also prepared using methods described elsewhere in the literature[6,12] in order to investigate the material-species-dependent variation in the Ar GCIB sputtering yield.

The valence bands and core levels of the organic composite films were analyzed *in situ* by combining PES with Ar GCIB sputtering (averaging 2500 Ar atoms/cluster). The 2 × 2 or 5 × 5-mm^2 raster and 5, 10, 15, or 20 kV acceleration used for Ar GCIB sputtering were modified during XPS (beam diameter: 100 μm). Changing from a 2 × 2- to a 5 × 5-mm^2 raster produced less than half of the original sputtering yield (*e.g.*, the 2 × 2- and 5 × 5-mm^2 rasters produced 2–4 and 1.5–2.5 nm/min sputtering yields, respectively, at 5 keV acceleration).

The molecular depth profile and planar atomic compositions of the as-deposited (as-dep.) and Ar-GCIB-sputtered organic composite films were preferentially examined based on XPS mapping microanalysis, which offers a spatial resolution of 7.5 μm and an effective analysis range of 500 × 500 μm^2. Further, HR-OM, HR-AFM, and HR-SEM were used to investigate the morphologies of the CNT and MWCNT/PEDOT:PSS films below the submicron scale before and after Ar GCIB sputtering.

3. Results and discussion

The HR-SEM images in Figure 1 show the cross-sections and morphologies of the as-dep. SWNT ((a) and (b)) and MWCNT ((c) and (d)) films, respectively. The CNT films both clearly show highly entangled CNT chains under the surfactant, suggesting that the organic matrix covered almost all the CNT chains in the dried spin-coated films and that the material was distributed differently between the top and bottom of the films.

The SWNT film structure can be simplified based on the SEM images in Figures 1 (a) and (b), as shown in the schematic diagrams in Figure 2 (a). On the whole, the SWNT bundles

including various sizes of chain aggregates were randomly spread out over the SiO_2/Si substrate and were densely packed together. The surfactant entirely wrapped around entangled SWNT networks and the outer faces of individual SWNT strands, forming a membrane crust. Analogous to common CNT ink consisting of an organic surfactant and CNTs, the SWNT ink used in this work was comprised of sodium dodecyl sulfate (SDS) and SWNT strands, as shown in Figure 2 (b). Except for a tiny proportion of minor component elements (*e.g.*, sulfur, oxygen, and sodium), both inks are hydrocarbon compounds containing alkyl backbones sp^3 (-C-C-) of surfactant and graphitic backbones sp^2 (-C=C-) of SWNT. Despite their similar atomic compositions, their XPS spectra clearly showed different chemical states in the C 1*s* core levels, depending on whether their carbon atoms were sp^2- or sp^3- hybridized.[6,11]

Until recently, XPS depth profiles could not provide reliable information about the molecular distribution of conventionally sputtered organic composite films owing to Ar-ion-bombardment-damage-induced chemical transition. Our group combined Ar GCIB sputtering with PES to study the chemical/electrical structures of organic layered films, thereby enabling the molecular distributions of organic composite films to be designed and characterized without sacrificing the atomic concentration and chemical structure.[6,7,11] A schematic diagram summarizing the experimental concept used to investigate the molecular distributions of the organic composite films is shown in Figure 3.

The XPS depth profiles for the SWNT and MWCNT films were preferentially measured during conventional Ar ion sputtering. Figure 4 shows the changes in the atomic concentrations of the (a) SWNT and (b) MWCNT films on the SiO_2/Si substrates and the relative ratios of the sp^2- and sp^3-hybridized carbon atoms in the (c) SWNT and (d) MWCNT films plotted as functions of sputtering time. The SWNT and MWCNT films both showed atomic concentrations different from their original ones after the initial 2-min sputtering cycle,

as shown in Figures 4 (a) and (b). Ar ion bombardment damaged the surface by replacing or breaking relatively unstable covalent bonds containing sulfur, oxygen, or nitrogen, thereby producing an abnormally high carbon concentration.[6] Furthermore, the CNT films did not show any obvious change in the relative ratios of the sp^2- and sp^3-hybridized carbon atoms with increasing sputtering time (Figures 4 (c) and (d)), although the SEM images show different molecular distributions for the top and bottom regions of the films.

However, combining PES with Ar GCIB sputtering provided trustworthy data on the real molecular distributions of the organic composite films. In fact, notwithstanding the highest acceleration voltage (20 kV) among the predetermined settings, the XPS depth profiles in Figure 5 obviously reflect the molecular distributions of the SWNTs and the surfactant for the entire depth of the SWNT film. On the basis of the XPS depth profiles in Figures 5 (a)-(e), more sodium and sulfur components, the constituent elements of the surfactant, were observed near the air-exposed surface region of the SWNT film, and the peak areas for Na^+ (1071 eV in the Na 1*s* core level) and S-O_x (167.6 eV in the S 2*p* core level) chemical states simultaneously decreased as the XPS measurement point approached the SWNT/SiO_2 interface region. Further, the peak corresponding to the C 1*s* core level became less intense as the peaks corresponding to the SiO_2 chemical states in the O 1*s* and Si 2*p* core levels simultaneously intensified. However, the C 1*s* core level, shown in Figure 5 (a), distinctly presents the main sp^3-to-sp^2 transition (*i.e.*, 284.8 to 284.0 eV) of the carbon atoms in the films with increased sputtering time. Therefore, the relatively high composition of surfactant molecules at the exterior surface of the SWNT films can be specifically characterized based on this interpretation of the XPS depth profile.

The XPS depth profiles for the as-dep. SWNT/SiO_2/Si structures were then measured during Ar GCIB sputtering operated at (a) 5, (c) 10, and (e) 20 kV acceleration, as shown in Figure 6. Except for the detailed atomic compositions, all the XPS depth profiles changed independent

of the acceleration voltage. The compositions of the main surfactant components (*e.g.*, carbon, sodium, and sulfur) decreased while the silicon and oxygen compositions approached the SiO_2 substrate component ratio with increasing sputtering time. The C 1*s* core level spectra were also used to investigate the effect of sputtering time on the relative ratios of sp^2- and sp^3-hybridized carbon atoms in the films sputtered at (b) 5 (d) 10, and (f) 20 kV. Of course, the XPS depth profiles generated during low-acceleration-voltage Ar GCIB sputtering provide more detail about the change in the relative ratios of the sp^2- and sp^3-hybridized carbon atoms than those generated during high-acceleration-voltage sputtering; however, the transition behaviors shown in Figures 6 (b), (d), and (f) exactly correspond to the respective atomic concentrations shown in Figures 6 (a), (c), and (e). The C 1*s* core level for the as-dep. SWNT films prepared without Ar GCIB sputtering mostly consisted of sp^3-hybridized carbon atoms owing to air-contamination and the surfactant. The relative ratio of sp^2- to sp^3-hybridized carbon atoms, on the other hand, gradually increased with increasing sputtering time until eventually the core levels of the films mostly consisted of sp^2-hybridized carbon atoms, as shown in Figures 6 (b), (d), and (f).[6,11]

Figures 7 (a)-(c) show the deconvoluted peaks of the of C 1*s* core levels for the as-dep. films and for the films sputtered at 5, 10, or 20 kV acceleration for various lengths of time. The XPS spectrum for the SWNT film showed peaks corresponding to the -C-O-, -C-C-, and -C=C- functional groups, and the difference between the chemical states of the surfactant and SWNT C 1*s* core levels enabled the depth-dependent molecular distributions to be investigated.[11,12] The area ratio of the peak corresponding to the sp^2-hybridized carbon atoms to the entire spectrum for the C 1*s* core level directly corresponds to the chemical composition of the SWNT film at each depth; therefore, comparing the profiles for the peak areas of the sp^3- and sp^2-hybridized carbon atoms could provide the exact distribution of the sp^3- and sp^2-hybridized carbon atoms in the surfactant and SWNT strands.

XPS mapping was also used to determine the spatial molecular distributions of the as-dep. film and the films sputtered under various conditions. Figures 8 (a)-(d) show the XPS mapping images (500 × 500 μm^2), assembled from individual 10-μm RGB (red: O; green: C; and blue: Si) atomic component units, corresponding to the HR-OM images of the as-dep. film and the films sputtered under the various conditions. From the XPS depth profiles, the surface region of the as-dep. SWNT film was fully covered with surfactant mainly consisting of carbon and a small percentage of oxygen; therefore, the corresponding XPS mapping image was yellowish green. However, carbon aggregates were irregularly distributed on the SiO_2 (violet) substrate surface during sputtering, as shown in Figures 8 (b) and (c), suggesting that the SWNT strands were not uniformly well-blended but strongly entangled in SWNT clusters under the surfactant materials in the SWNT film. Further, the XPS mapping image in Figure 8 (d) still shows evidence of the SiO_2 substrate (violet) after the films had been sufficiently sputtered to remove the SWNT clusters.

The corresponding micromorphologies (5 × 5 μm^2) of the sputtered SWNT films were also examined. As in the HR-OM and XPS mapping images, the surfactant and SWNTs appear to be nonuniformly distributed in the HR-AFM images in Figures 9 (a)-(d); however, the material structures can be precisely distinguished in the corresponding HR-AFM images of the Ar GCIB sputtered SWNT films. As in the HR-SEM images in Figures 1 (a) and (b), the surface of as-dep. SWNT film in Figure 9 (a) appears fully covered with a smooth surfactant matrix and shows a highly entangled structure consisting of SWNT strands at the bulk region (Figures 9 (b) and (c)). Only some SWNT and surfactant fragments remained on the SiO_2 substrate upon further sputtering, as shown in the HR-AFM image in Figure 9 (d).

XPS depth profiles were subsequently generated for a single 50-nm-thick PEDOT:PSS thin film and the ~20-nm-thick, almost-surfactant-free, H_2SO_4-treated SWNT film to investigate whether the organic species in the SWNT film produced different sputtering yields.[12]

Although the PEDOT:PSS and H_2SO_4-treated SWNT showed different thicknesses, the depth profiles in Figures 10 (a) and (b) did not show any noticeable material-species-dependent difference in the sputtering yield. The PEDOT:PSS and H_2SO_4-treated SWNT films were fully removed after 2 and 1 min of sputtering at 20 kV and 5 × 5 mm^2, respectively, leaving mainly the SiO_2 substrates in common. However, as in the XPS depth profile, the UPS depth profile for the SWNT film showed an entirely different valence band structure, depending on which sputtering method had been used, as shown in Figures 10 (c) and (d). The C=O, C-O, S=O, and S-O reactive functional groups in organic materials are easily degraded or replaced by stabler ones such as C-H, C-S, C-C, and C=C during Ar ion sputtering, as previously reported elsewhere in the literature.[6,7,11] In other words, Ar monomer ion beam bombardment transforms the chemical states including the valence band structure of organic materials into that of carbon black or graphitic compounds. Therefore, abnormal sp^2 (π-π*) hybrid states had formed near the Fermi level of the Ar-ion-sputtered SWNT film, and even the area of their domains gradually increased with increasing sputtering time, as shown in Figure 10 (c). The original valence band structure of the SWNT film, on the other hand, was well preserved during sputtering. The chemical states near the Fermi energy were independent of the insulating surfactant but highly dependent on the sp^2 (π-π*) hybrid states of the metallic SWNT strands. Therefore, the relative areas of those states incrementally increased depending on the cyclic-sputtering-induced decrease in the surfactant-to-SWNT ratio, as shown in Figure 10 (d). The molecular distributions of the surfactant and SWNT could also be approximated by investigating the change in the area, as shown in Figure 10 (d).

4. Conclusions

XPS combined with Ar GCIB sputtering was used to determine the molecular configurations of SWNT and MWCNT organic composite films. In contrast to Ar ion

sputtering, Ar GCIB sputtering did not critically damage the chemical states or the morphological molecular structure of the organic films. Rigorous analysis of the XPS/UPS spectra and AFM/SEM images of the SWNT films showed that the variation in the chemical structures with increasing Ar GCIB sputtering time fully corresponded to the vertical molecular configurations of the organic composite films. Our method can be used to determine the molecular configurations of organic composite films without critically damaging their chemical states or their morphological molecular structures.

References

1. S. W. Rhee and D. J. Yun, *J. Mater. Chem.*, 2008, **18**, 5437.

2. H. Ma, H. L. Yip, F. Huang and A. K. Y. Jen, *Adv. Funct. Mater.*, 2000, **20**, 1371.

3. D. J. Yun and S. W. Rhee, *J. Mater. Chem.*, 2010, **20**, 9754.

4. B. Fan, X. Mei, K. Sun and J. Ouyang, *Appl. Phys. Lett.*, 2008, **93**, 143102.

5. A. M. Ektessabi and S. Hakamata, *Thin solid films*, 2000, **377**, 621.

6. D. J. Yun, C. Jung, H. I. Lee, K. H. Kim, Y. K. Kyoung, A. Benayad and J. Chung, J. Electrochem. Soc. **159**, H626 (2012).

7. D. J. Yun, J. Chung, C. Jung, K. H. Kim, W. Baek, H. Han, B. Anass, G. S. Park and S. H. Park, *J. Appl. Phys.*, 2013, **114**, 013703.

8. E. Vitoratos, S. Sakkopoulos, E. Dalas, N. Paliatsas, D. Karageorgopoulos, F. Petraki, S. A. Kennou, Org. Electron., 2009, **10**, 61.

9. N. Koch, A. Volmer and A. Elschner, Appl. Phys. Lett., 2007, **90**, 043512.

10. T. Miyayama, N. Sanada, S. R. Bryan, J. S. Hammond and M. Suzuki, Surf. Interface Anal. 2010, **42**, 1453.

11. D. J. Yun, J. Chung, C. Jung, Y. Chung, S. Kim, S. Lee, K. H. Kim, H. Han, G. S. Park and S. H. Park, *J. Appl. Phys.*, 2013, **114**, 094510.

12. D. J. Yun, J. M. Kim, H. Ra, S. J. Byun, H. S. Kim, G. S. Park, S. H. Park and S. W. Rhee, *Org. Electron.*, 2013, **14**, 2962.

Figure captions

Figure 1 HR-SEM images of cross-sections and morphologies of as-deposited SWNT (a) and (b) and MWCNT (c) and (d) films, respectively.

Figure 2 Schematic diagrams showing (a) as-deposited SWNT film structure consisting of surfactant and SWNT bundles nonuniformly spread out and densely packed together and (b) distinguishable chemical states of hybridized carbon atoms in surfactant and SWNT.

Figure 3 Schematic diagram for experimental concept devised by combining XPS depth profile analysis with Ar GCIB sputtering and used to investigate molecular distributions of organic composite films.

Figure 4 XPS depth profiles generated for SWNT and MWCNT films during conventional Ar ion sputtering, providing information about changes in atomic concentrations (a) SWNT and (b) MWCNT films on SiO_2/Si substrates and relative ratios of the sp^2- and sp^3-hybridized carbon atoms in (c) SWNT and (d) MWCNT films plotted as functions of sputtering time.

Figure 5 XPS depth profiles for (a) C 1*s*, (b) S 2*p*, (c) Na 1*s*, (d) O 1*s*, and (e) Si 2*p* core levels generated while sputtering SWNT film onto SiO_2/Si substrate.

Figure 6 (a), (c), and (e) XPS depth profiles and (b), (d), and (f) relative compositions of sp^3- and sp^2-hybridized carbon atoms in SWNT/SiO_2/Si structures of films sputtered at 5, 10, and 20 kV acceleration.

Figure 7 Deconvoluted peaks (attributed to -C-O-, -C-C-, and -C=C- functional groups) for C 1*s* core levels of SWNT films sputtered at (a) 5, (b) 10, and (c) 20 kV acceleration for various lengths of time.

Figure 8 XPS mapping images (500 × 500 μm^2), assembled from individual 10-μm RGB (red: O; green: C; and blue: Si) atomic component units, corresponding to HR-OM images of

(a) as-dep. SWNT film and SWNT films sputtered (b) at 5 kV for 20 min, (c) at 10 kV for 10 min, and (d) at 20 kV for 10 min.

Figure 9 AFM images (5×5 μm^2) of (a) as-dep. SWNT film and SWNT films sputtered (b) at 5 kV for 20 min, (c) at 10 kV for 10 min, and (d) at 20 kV for 10 min.

Figure 10 Referential XPS depth profiles for individual (a) organic polymer (PEDOT:PSS) and (b) surfactant-removed (H_2SO_4-treated SWNT) CNT films. Apparently contradictory results obtained for UPS depth profiles for SWNT films are owing to (c) Ar ion and (d) Ar GCIB sputtering.

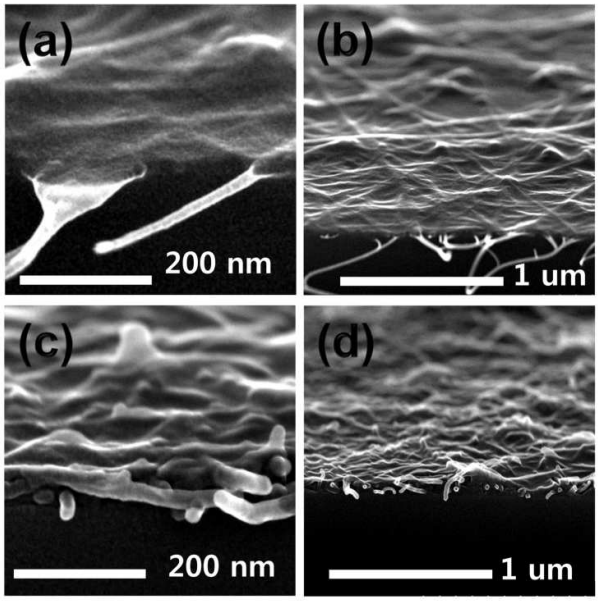

Figure 1. Yun et al.

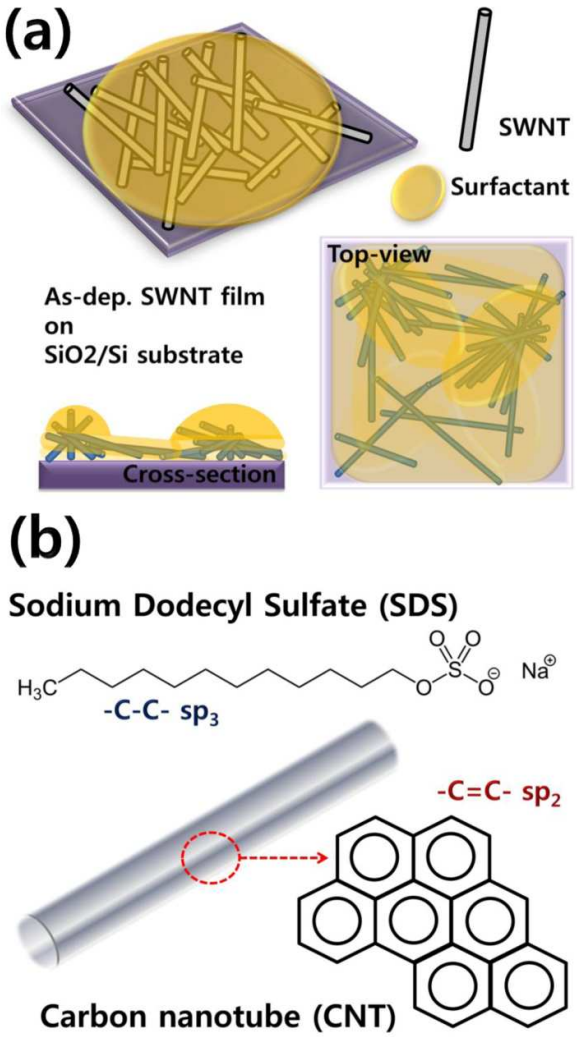

Figure 2. Yun et al.

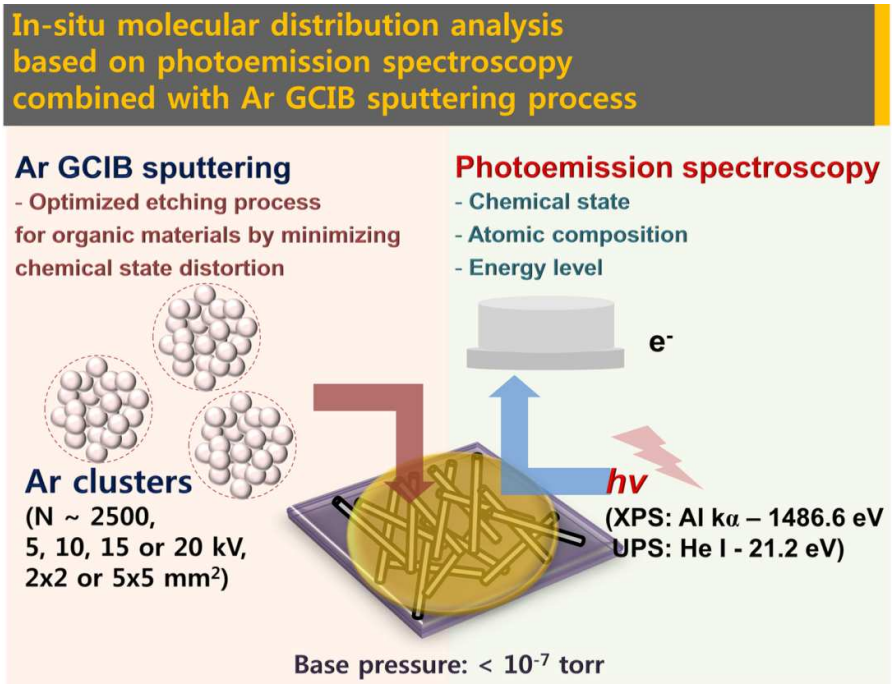

Figure 3. Yun et al.

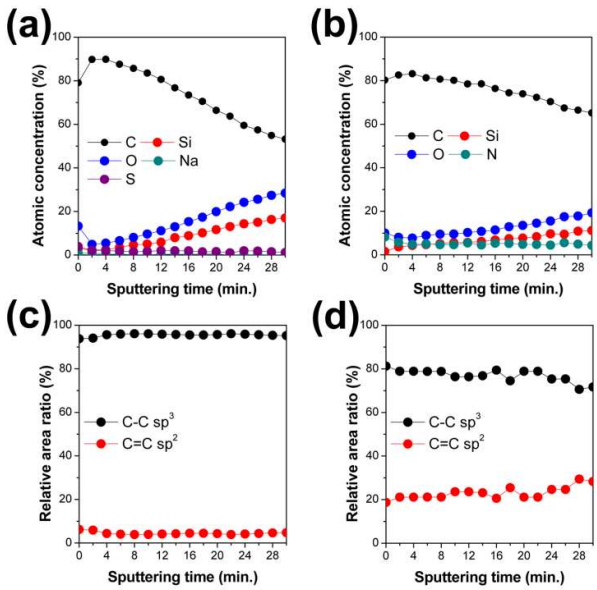

Figure 4. Yun et al.

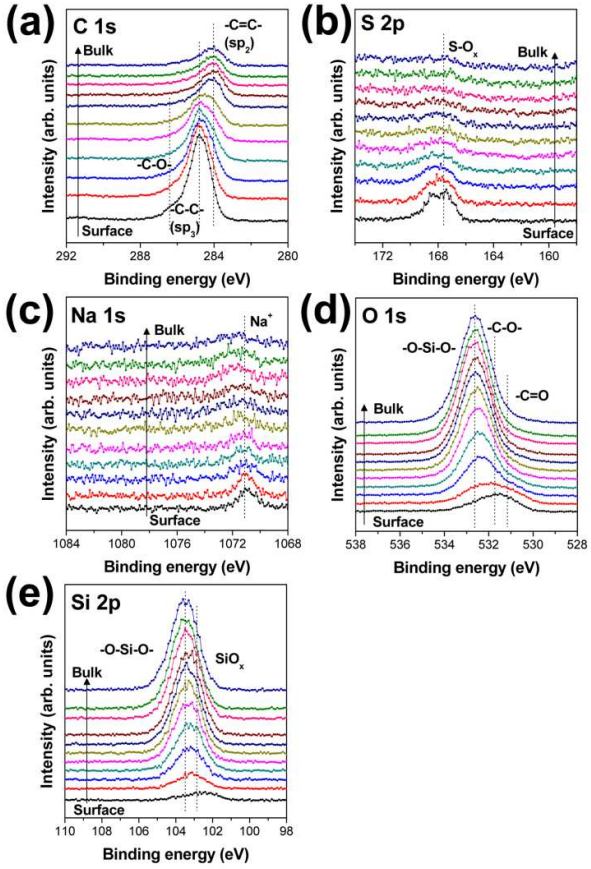

Figure 5. Yun et al.

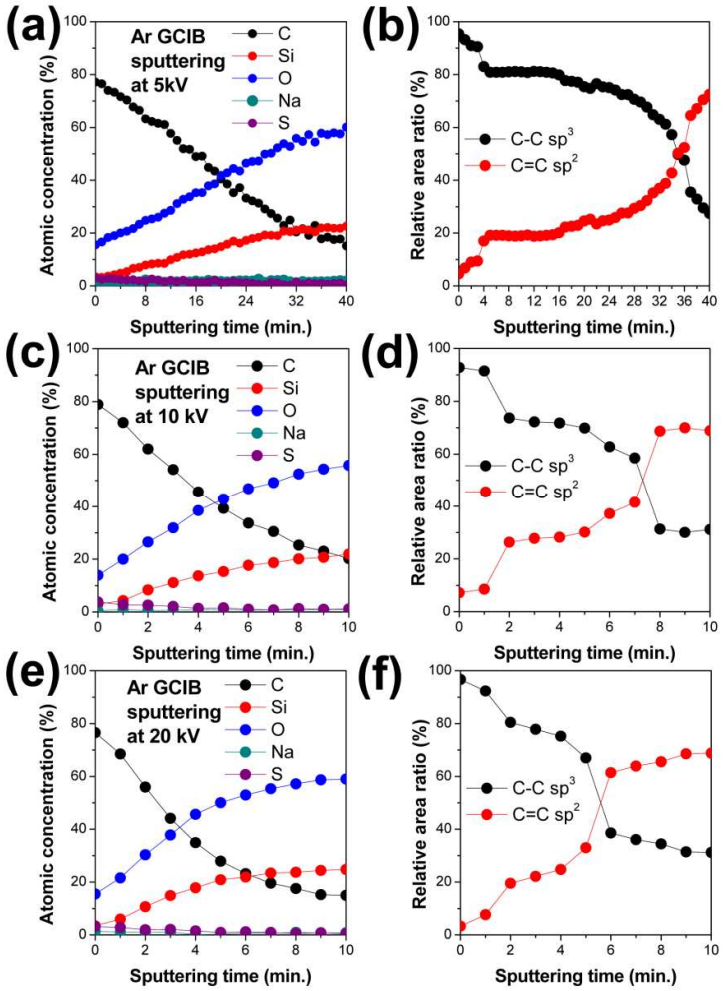

Figure 6. Yun et al.

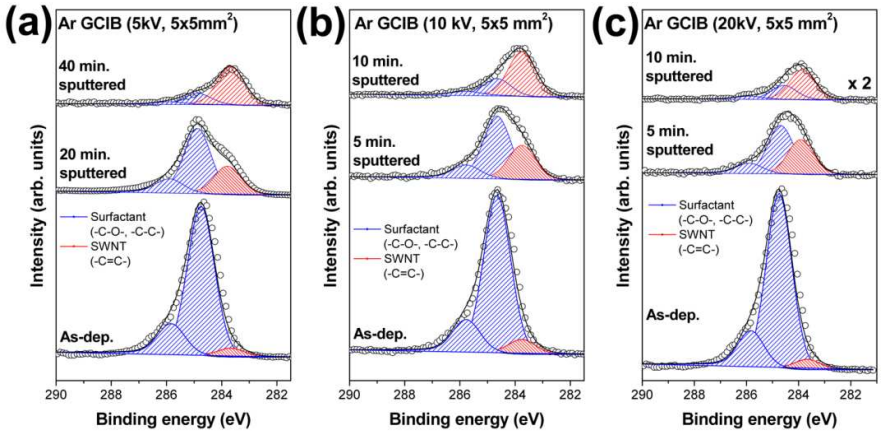

Figure 7. Yun et al.

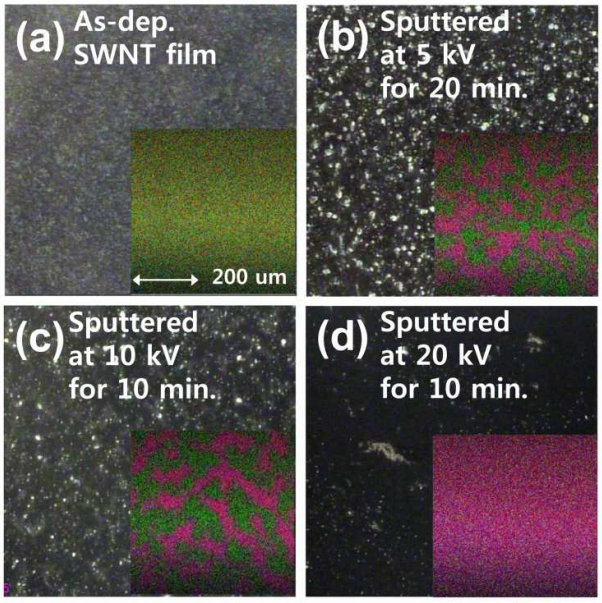

Figure 8. Yun et al.

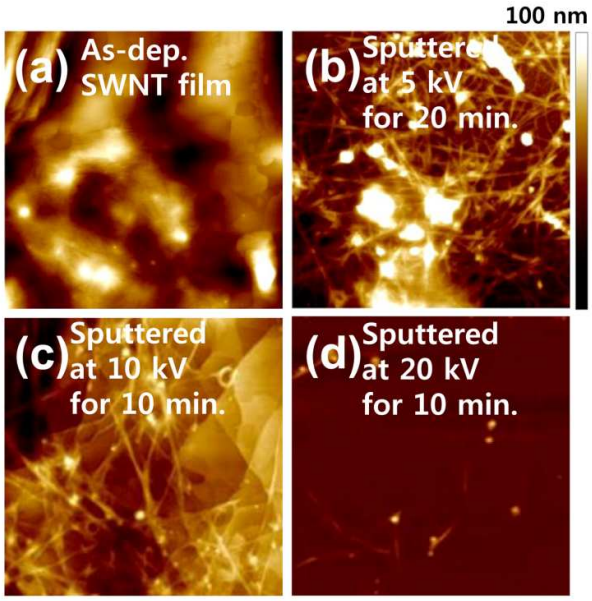

Figure 9. Yun et al.

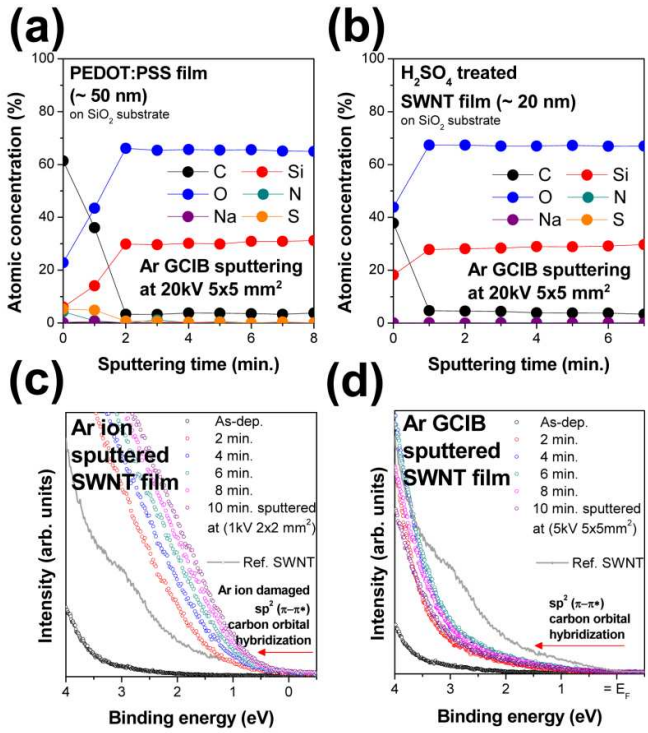

Figure 10. Yun et al.

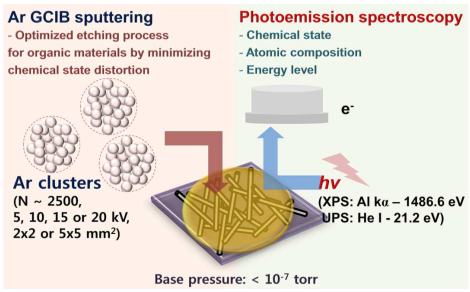

In-situ molecular distribution analysis based on photoemission spectroscopy combined with Ar Gas Cluster Ion Beam sputtering process